

8

Conf-9110259-1

GA-A20682

CONFIDENTIAL

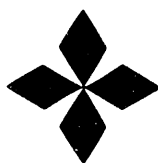
OCT 0 1991

# AN X-POINT ERGODIC DIVERTOR

by

M.S. CHU, T.H. JENSEN, R.J. La HAYE,  
T.S. TAYLOR, and T.E. EVANS

OCTOBER 1991



**GENERAL ATOMICS**

DISTRIBUTION OF THIS DOCUMENT IS UNLIMITED

## DISCLAIMER

This report was prepared as an account of work sponsored by an agency of the United States Government. Neither the United States Government nor any agency thereof, nor any of their employees, makes any warranty, express or implied, or assumes any legal liability or responsibility for the accuracy, completeness, or usefulness of any information, apparatus, product, or process disclosed, or represents that its use would not infringe privately owned rights. Reference herein to any specific commercial product, process, or service by trade name, trademark, manufacturer, or otherwise, does not necessarily constitute or imply its endorsement, recommendation, or favoring by the United States Government or any agency thereof. The views and opinions of authors expressed herein do not necessarily state or reflect those of the United States Government or any agency thereof.

# AN X-POINT ERGODIC DIVERTOR

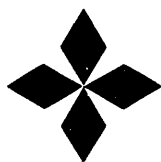
by

M.S. CHU, T.H. JENSEN, R.J. La HAYE,  
T.S. TAYLOR, and T.E. EVANS

This is a preprint of a paper presented at the IAEA  
Technical Committee Meeting on Research Using Small  
Tokamaks, October 3-8, 1991, Hefei and Huangshan  
City, People's Republic of China.

Work supported by  
U.S. Department of Energy  
Contract DE-AC03-89ER53277

GENERAL ATOMICS PROJECT 3468  
OCTOBER 1991



**GENERAL ATOMICS**  
**MASTER**

A handwritten signature or set of initials in black ink, appearing to be 'JMO'.

## An X-Point Ergodic Divertor

M.S. CHU, T.H. JENSEN, R.J. LA HAYE, T.S. TAYLOR, and T.E. EVANS

General Atomics

San Diego, California 92186-9784, U.S.A.

### *Abstract*

A new ergodic divertor is proposed. It utilizes a system of external ( $n = 3$ ) coils arranged to generate overlapping magnetic islands in the edge region of a diverted tokamak and connect the randomized field lines to the external (cold) divertor plate. The novel feature in the configuration is the placement of the external coils close to the X-point. A realistic design of the external coil set is studied by using the field line tracing method for a low aspect ratio ( $A \simeq 3$ ) tokamak.

Two types of effects are observed. First, by placing the coils close to the X-point, where the poloidal magnetic field is weak and the rational surfaces are closely packed, only a moderate amount of current in the external coils is needed to ergodize the edge region. This ergodized edge enhances the edge transport in the X-point region and leads to the potential of edge profile control and the avoidance of edge localized modes (ELMs). Furthermore, the trajectories of the field lines close to the X-point are modified by the external coil set, causing the hit points on the external divertor plates to be randomized and spread out in the major radius direction. A time-dependent modulation of the currents in the external ( $n = 3$ ) coils can potentially spread the heat flux more uniformly on the divertor plate avoiding high concentration of the heat flux.

## Contents

Abstract . . . . .	iii
1. Introduction . . . . .	1
2. A "Helical Coil Set" in DIII-D Geometry . . . . .	5
3. The "Window Pane" Coil . . . . .	15
4. A Combination of the Coils . . . . .	19
5. Conclusions . . . . .	21
6. Acknowledgments . . . . .	23
7. References . . . . .	25

## *Figures*

1. Physical layout of the DIII-D tokamak in the poloidal cross-section . . . . .	6
2. Fourier amplitudes of the perturbation magnetic field . . . . .	7
3. Perturbation radial and poloidal magnetic field strength . . . . .	8
4. Puncture plot of a collection of field lines . . . . .	10
5. Length of the field lines as a function of their starting position . . . . .	11
6. The length of the lost field lines replotted as a function function of the toroidal and poloidal angle of their hit points . . . . .	13
7. Fourier amplitudes of the perturbation field . . . . .	16
8. The length of the lost field lines due to the effect of the window pane coils plotted as a function of the toroidal and poloidal angle of their hit points . . . . .	17
9. Length of the field lines as a function of their starting position on the outboard midplane . . . . .	20

## 1. Introduction

The edge and divertor plasma behavior has long been recognized as major issues of the thermonuclear research. In present day tokamaks, sharp edge gradients result from enhanced edge confinement in H-mode and lead to the occurrence of edge localized modes (ELMs) [1]. One of the difficulties in future fusion reactors is the prolonged concentration of heat flux along the divertor channel to the divertor plates [2]. It will lead to copious impurity production at the divertor plate and the subsequent impurity backflow into the main plasma. It is therefore desirable to have a method to allow us provide control to the edge and divertor region of the magnetic configuration.

Up to now various innovative ideas have been proposed to alleviate the problems of a hot plasma edge interfacing with the external cold wall. These include the ergodic divertor [3] and the axisymmetric X-point sweep [4]. In the ergodic divertor, a system of external coils are arranged to generate overlapping islands in the edge region of the plasma and connect the stochastic field lines to the external wall. Rapid parallel transport along field lines in this stochastic layer will enhance the effective perpendicular diffusion, leading to a cooled plasma edge with increased radiated power. The increased particle flux to the walls produces a larger neutral influx which, if ionized within the stochastic layer, increases the local density. Since the penetration probability falls exponentially with density, an increase in the neutral screening factor is triggered and impurity neutrals are ionized closer to the vessel walls. Thus, the radiation profiles move radially outward and increase in the stochastic layer. The enhanced outflux of the plasma further entrains the impurity ions and prevent them from entering the plasma. In the axisymmetric X-point sweep, the X-point location is swept in time to prevent the sustained heat flux at a fixed location on the divertor floor. This is expected to circumvent the concentrated heat load problem of the divertor plates.

Ergodic boundary layers have already been implemented on various tokamaks, notably TEXT [5], Tore Supra [6], and JFT-2M [7]. Both TEXT and Tore Supra are circular tokamaks. Activation of the ergodic perturbation coils has been observed

to lower the edge temperature and temperature gradient in the stochastic layer and reduce the carbon impurity concentration in the core plasma. JFT-2M is a noncircular tokamak. During its H-mode operation, activation of the ergodic divertor has been observed to enlarge its operational space of the ELMy discharges. Therefore, the ergodic boundary layer provides an important method of impurity and ELM control. The axisymmetric X-point sweep has been proposed and tested in DIII-D [8]. Up to a factor of two reduction in the peak surface temperatures on the divertor floor have been observed.

In all the previous ergodic layer experiments, the helical fields are produced either by full poloidal coils with a  $\cos\theta$  modulation or by coils placed on the large major radius side of the plasma cross-section. This could be the optimal design for the circular tokamak. In the circular tokamak, the shear of the safety factor  $q$  profile is weaker than that of a noncircular tokamak. The resonant surfaces are therefore further apart. The magnetic islands needed to obtain overlap are therefore larger in radial size, and the resultant stochastic layer is wider. It is also more likely for the ergodic field to penetrate deeper into the confinement ( $q < 2$ ) region.

In a noncircular diverted tokamak, the  $q$  value near the separatrix varies as  $\ell n(\psi - \psi_s)$ , where  $\psi_s$  is the poloidal flux function value at the separatrix. The trajectory of the magnetic field in a flux surface based coordinate system satisfies the equation

$$\frac{d\psi}{R B_p \tilde{B}_\psi} = \frac{d\ell_p}{B_p + \tilde{B}_p} = \frac{R d\phi}{B_\phi + \tilde{B}_\phi} ,$$

where quantities with a tilde are the perturbed quantities. If, as a first approximation, we ignore the perturbed quantities relative to the unperturbed ones, the perturbation in  $\psi$  of a flux line is then given by

$$\delta\psi = \int_{\text{unperturbed trajectory}} \tilde{B}_\psi R d\ell_p ,$$

It is observed that near the X-point, where the poloidal length is elongated, the same amount of  $\tilde{B}_\psi$  will produce a larger perturbation in the excursion of the field line trajectory than in a circular tokamak.

The hit points of the lost field lines from the edge of the plasma depend mostly on their trajectory when they pass through the X-point region. Over this region, the equilibrium poloidal field is weak. An  $n \neq 0$  perturbation field of moderate size can easily produce a non-axisymmetric modulation.

In this paper, we propose an improved arrangement of the the ergodic divertor coils for a diverted tokamak. In Section 2, we show an example of such an arrangement for DIII-D. A system of  $n = 3$  external coils is designed to be placed around the X-point of a lower single null equilibrium. The resultant field line topology is studied with different coil currents. We show that the coil currents could have a rich harmonic content and will resonate with flux lines at the plasma edge. With 5 kA turns of current in the ergodic coils, a thin layer  $\sim 4$  cm in width around the separatrix is ergodized for a plasma with  $\sim 1$  MA of plasma current. The hit points on the divertor floor are also broadened to 8 cm in width on the outboard side and 4 cm in width on the inboard side. In Section 3, the effect of one special unit in the above coil set, which takes the shape of a set of “window pane” coils placed on the divertor floor, is studied. It is found that exciting this set alone, generates a very peaked, low harmonic content and localized magnetic field perturbation at the separatrix. It thus generates negligible ergodic effect for field lines around the separatrix. With 37.5 kA current in the coils, a sizable excursion of the hit points on the divertor floor is generated. In Section 4, a combination of the effect of currents in the first and second sets is used to show that a reasonable range of field lines around the separatrix may be ergodized and at the same time the hit points on the divertor floor can have a large excursion. Thus, a proper combination of currents in the helical and the window pane coils will allow us to control the edge field line diffusivity and their hit points on the floor can have a large excursion. A brief conclusion with discussions is given in Section 5.

## 2. A "Helical Coil Set" in DIII-D Geometry

To show the effect of an X-point ergodic divertor coil set on a realistic diverted tokamak, we use as example its implementation on DIII-D. In the following, all the physical dimensions used are for the DIII-D geometry and it could be easily scaled or modified for other similar diverted configurations.

Shown in Fig. 1 is the physical layout of the DIII-D tokamak in the poloidal cross-section. The helical coil is shown and marked as circles with connected current carrying segments. Starting from the bottom floor, it is placed along the vacuum vessel upward toward the outboard midplane. It is noted that this placement of the coils, although being close to, is not symmetric with respect to the X-point and has been adjusted to be compatible with the existent DIII-D hardware. The geometric center of the plasma chamber is shown and the largest inscribed circle which fits into the chamber is marked as heavy dotted lines. A standard DIII-D single null configuration with its flux surfaces close to the separatrices are also traced by various symbols. These flux surfaces have  $q$  values of 2, 3, and 4, respectively. On the outboard midplane of the torus which goes through the magnetic axis, they are at a distance of 13.8, 5.3, and 2.8 cm from the separatrix, which is located at minor radius  $r = 0.668$  m. The X-point location is at height  $Z = -1.23$  m.

Shown in Fig. 2 are the Fourier amplitudes of the perturbation magnetic field on the inscribed circle shown in Fig. 1 for 5 kA-turns in the "helical coil." It is seen that on this circle the radial magnetic field has an  $n = 3$  component with a broad maximum peaked around  $m = 7$ . The maximum Fourier amplitude is around 2 G. The  $n = 9$  component is smaller by a factor of 3 with a similar spectral shape. For a more detailed study, the Fourier amplitudes on the actual unperturbed flux surfaces should be analyzed for their harmonic content. For noncircular cross-sectional shapes, the peak amplitude is expected to be higher for flux surfaces close to the separatrix. The harmonic content is also expected to be shifted in  $m$  number. For instance, the actual magnetic field strength along an unperturbed flux surface close to the separatrix is shown in Fig. 3 as a function of the poloidal angle  $\theta$ . 180 deg is at the inboard (in major radius direction) mid-plane and 360 deg is on the outboard midplane. Both

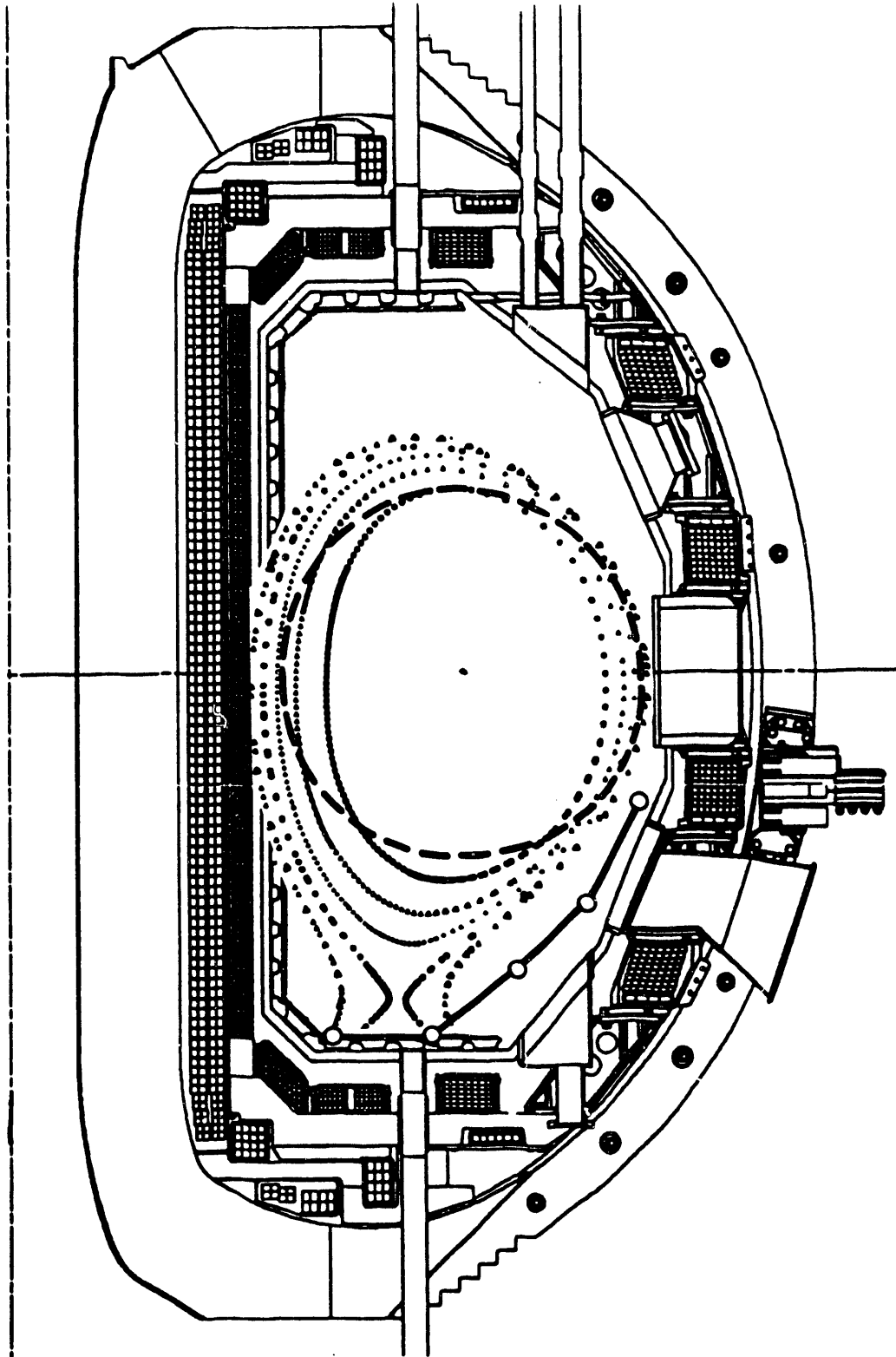


Fig. 1. Physical layout of the DIII-D tokamak in the poloidal cross-section. The location of the helical coil is shown and marked as circles with connected current-carrying elements. Starting from the bottom floor, it is placed along the vacuum vessel upward toward the outboard midplane. Shown are also an inscribed circle and standard DIII-D flux surfaces with  $q = 2, 3, 1$ .

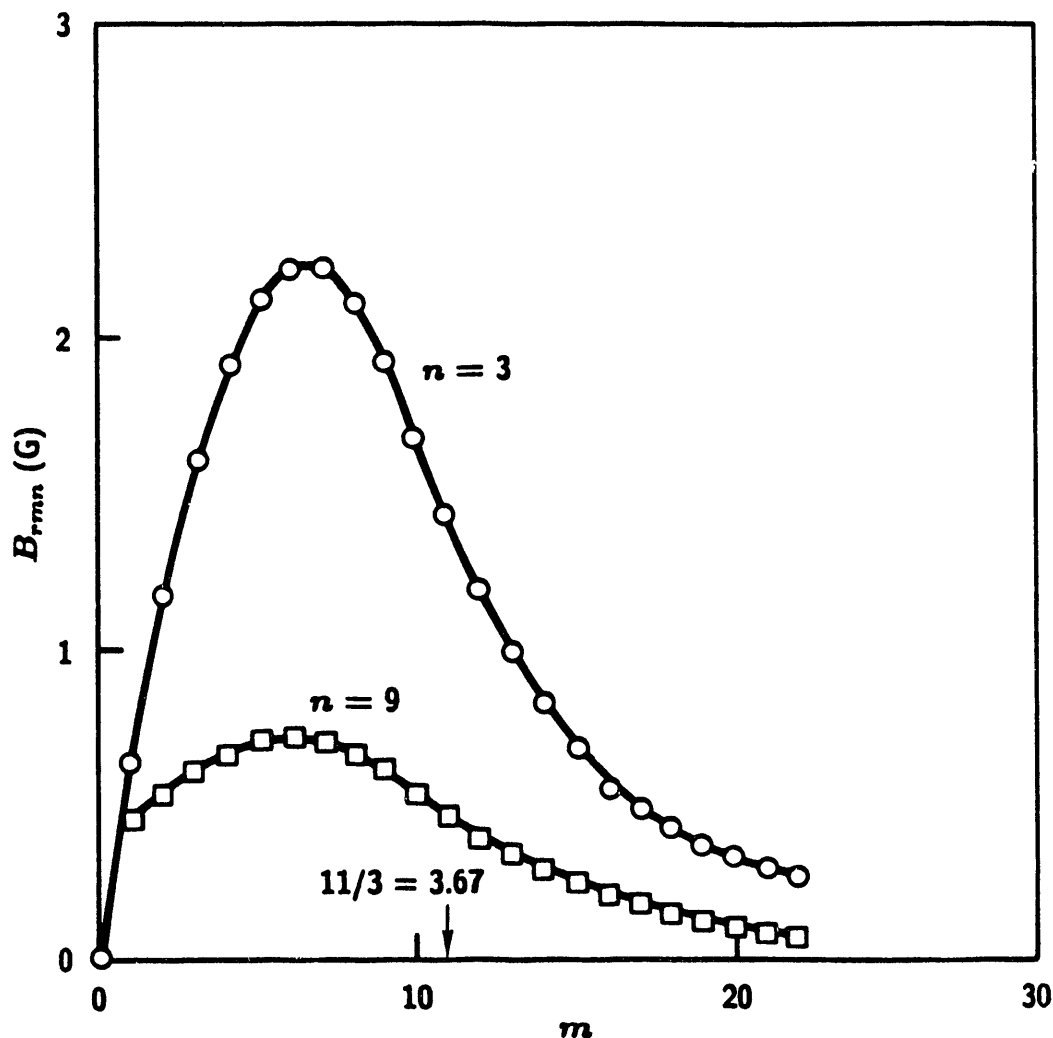


Fig. 2. Fourier amplitudes of the perturbation magnetic field produced by the helical coil on the circle shown in Fig. 1 as a function of poloidal mode number for  $n = 3$  and  $n = 9$ .

the perturbing radial and poloidal magnetic fields undergo large oscillations along the flux surface and it reaches 50 G at the maximum. Therefore, the main feature of this coil set is that it has a broad spectrum with a large perturbation field at the X-point region.

With the inclusion of the magnetic field due to the ergodic coils, the magnetic configuration becomes three dimensional in nature. Although there exist many good analytic theories based on perturbation of a axisymmetric equilibria or renormalized flux functions, in the truly stochastic field regime, only the field line tracing method [9] can give us a clear picture of the new configuration. The axisymmetric part of

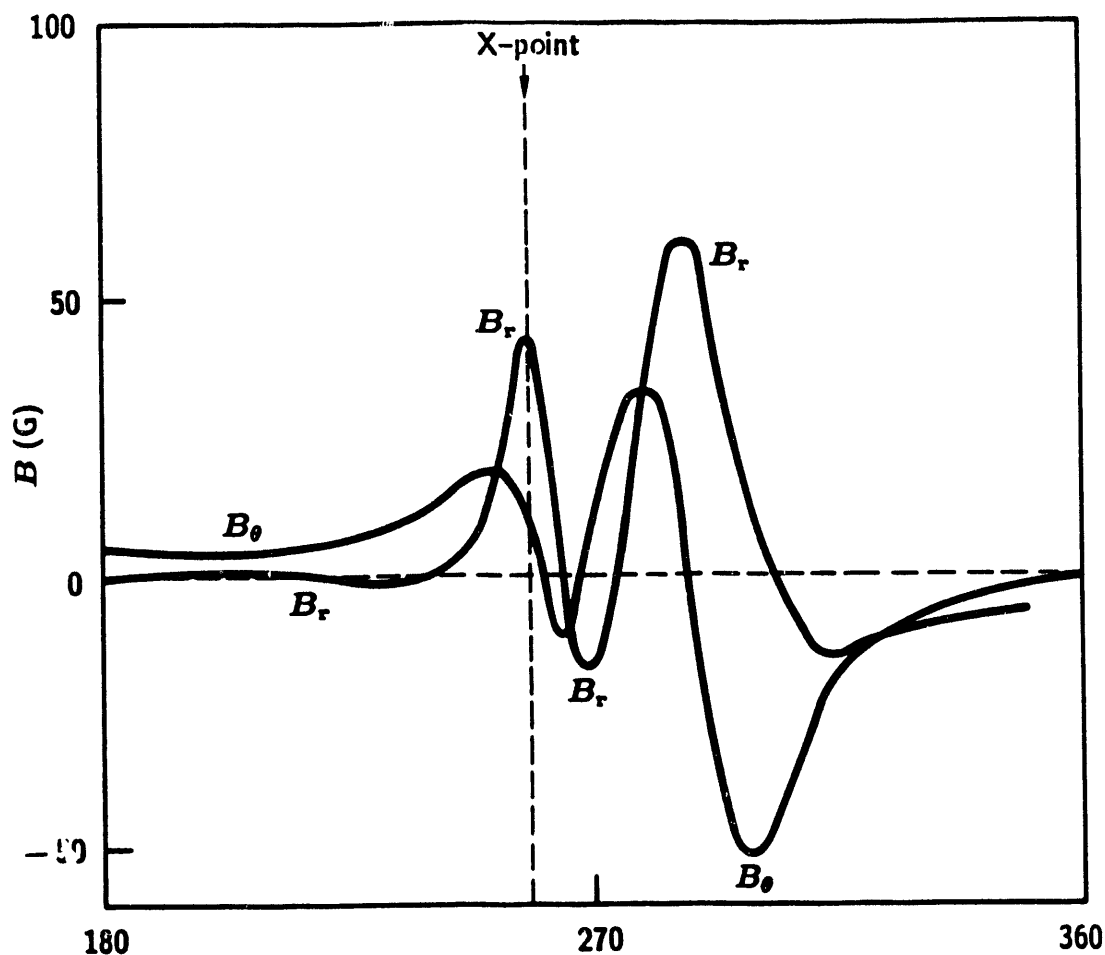


Fig. 3. Perturbation radial and poloidal magnetic field strength along an unperturbed flux surface close to the separatrix as a function of the poloidal angle  $\theta$ . 180 deg is at the inboard (in major radius direction) midplane and 360 deg is on the outboard midplane.

the equilibrium magnetic field has both a toroidal and a poloidal component. For simplicity, the toroidal field is assumed to have a vacuum field  $1/R$  dependence. The poloidal field is generated by using plasma current filaments and external vertical field coils to produce the desired plasma shape of a single null discharge. The toroidal current carried by the plasma is chosen to be 950 kA. The toroidal field strength of 1.3 T is adjusted to have  $q = 2$  and 3 surface locations that match a known DIII-D discharge. The total magnetic field used in the field line tracing consists of the axisymmetric equilibrium field together with magnetic field generated by currents in the ergodic divertor coils.

In the field line tracing picture, the volume of the plasma turns into a volume filled with interconnecting magnetic lines. Deep inside the plasma, the perturbation effect is small and the magnetic field lines are observed to trace out almost intact flux surfaces (some times with small islands). However, at the edge, due to the density of the resonant surfaces, there will be a stochastic region which is eventually connected to the external cold divertor plate. From the KAM theorem, it is known that there is a clear separation between the external 'stochastic lossy' region and the internal 'confined' region. Our objective here is to characterize this lossy region.

Details of the field line tracing results for 5 kA currents in the ergodic coils and with a maximum tracing of 100 toroidal circuits around the torus are shown in the following. One hundred toroidal turns is chosen because it corresponds to tens of collision mean free paths of the particles at the edge in the H-mode mode operation. Shown in Fig. 4 is the puncture plot of a collection of field lines starting from the outside midplane at toroidal angle  $\phi = 0$  and equally spaced in radius from 0.631 to 0.705. Plotted are three types of lines, the first is the solid lines which are the axisymmetric flux surfaces. The second type is the flux surface traced out by the unperturbed field lines. And, the third type is the field line trajectories traced out by the perturbed field lines. Approximately an equal number of field lines are started outside of the separatrix as are from inside. Trajectories of field lines started from outside of the separatrix are sparsely populated, showing they are promptly lost. The tilting of their radial extent shows the difference in their rotational transform angle. For field lines started from within the separatrix, the field lines generally would deviate from the original unperturbed flux surface. Although undiscernible from the figure due to the density of the lines traced, some of the lines will eventually cross the separatrix and enter the lossy region. This effect of the gradual loss of the field lines is best observed from Fig. 5. Plotted in this figure is the length of the field line as a function of their starting position on the outboard midplane shown on a logarithmic scale. The field lines are traced in the outboard going (shorter or clockwise as seen in Fig. 4) direction. Tracing of a line is stopped after it hit the divertor plate located at a location of  $Z = -1.33$  m. The field line length in  $\phi$  is the increment in toroidal angle at hit from its starting midplane location. The prompt loss lines would register as 0 or 1 in the figure. The scale increment is approximately 1.6, i.e., a field line registered as 2 would be 1.6 times longer than lines registered as 1. The field lines that are longer than 100 turns in length are registered as \*. It is seen that there is a

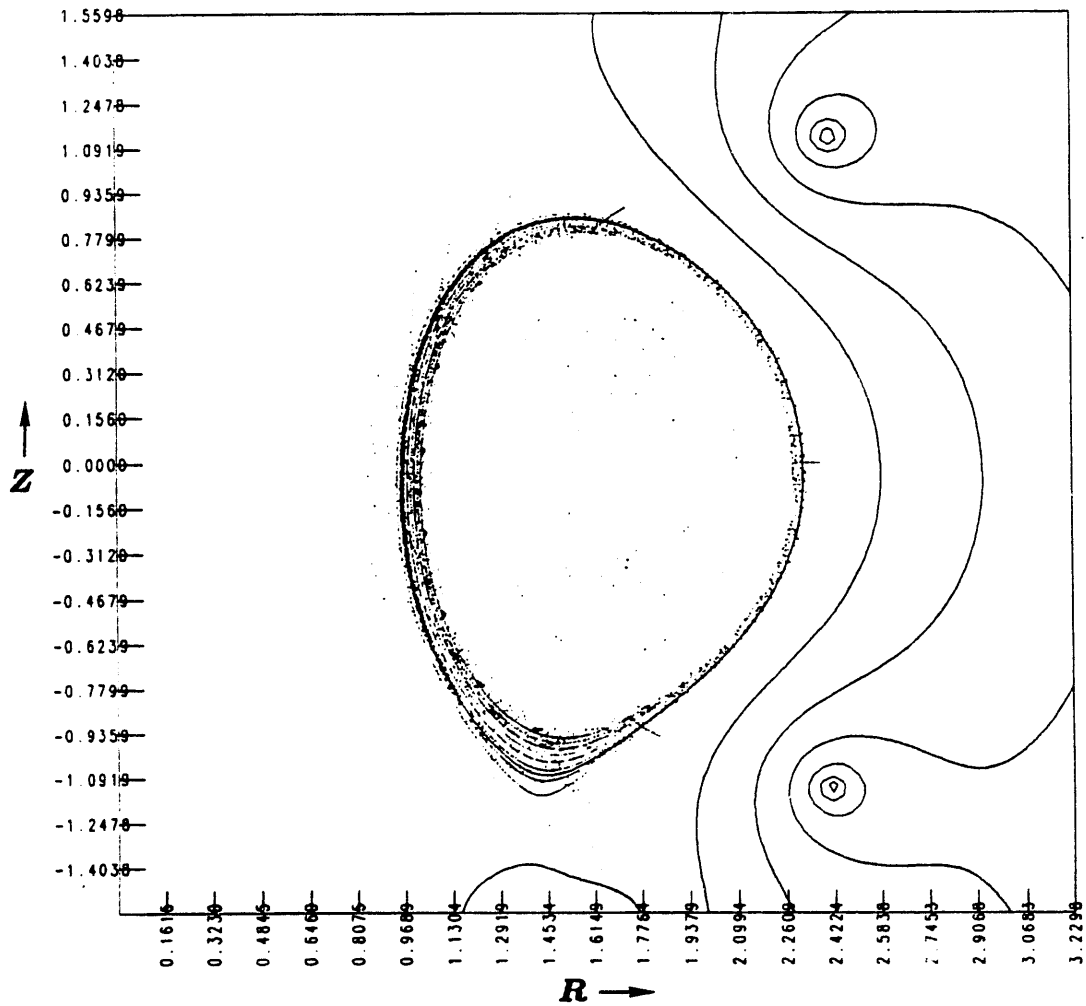


Fig. 4. Puncture plot of a collection of field lines starting from the outside midplane at a toroidal angle  $\phi = 0$  and equally spaced in radius from 0.631 to 0.705. The solid lines are axisymmetric flux surfaces not used in the tracing. As a reference, trajectories of field lines without the external perturbation fields are shown together with those with the perturbations from the external  $n = 3$  coils.

trend for the field line length to gradually increase as its starting position moves from close to the separatrix toward the plasma center. This trend is not monotonic but with certain imbedded randomness. The sinusoidal shaped locus of points marked as 1 may be regarded as the new plasma boundary. This is the plasma shape under the influence of the perturbation field. This pattern repeats every 120 deg in  $\phi$  for  $n = 3$ . The amplitude of this sinusoidal variation is proportional to the strength of the perturbation field. When we increase the maximum length of the field line that is traced, some of the field lines that are registered as \* will be lost. An increase of

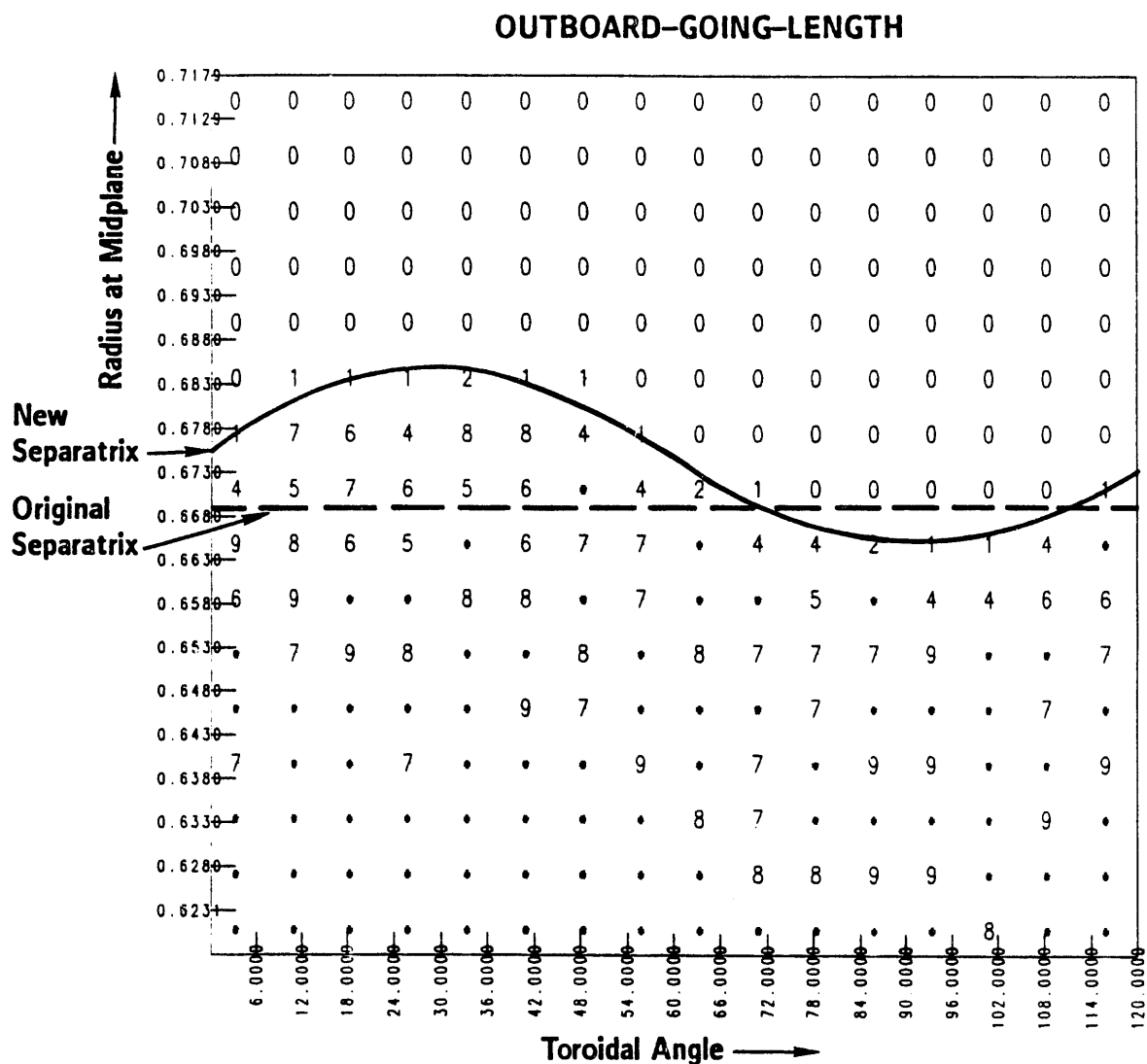


Fig. 5. Length of the field lines as a function of their starting position on the outboard midplane is shown on a logarithmic scale. The field lines are traced in the outboard going (shorter or clockwise as seen in Fig. 4) direction. The prompt loss lines are registered as 0 or 1. The field lines that are longer than 100 turns in length are marked as \*. The scale increment is approximately a factor of 1.6.

the field line length to four times as that shown in Fig. 5 indicates that none of the field lines deeper than 5 cm from the separatrix are lost.

The same group of field lines are also traced in the inboard going (longer) direction. A similar behavior is observed.

The length of the lost field lines can also be plotted as a function of the toroidal and poloidal angle of their hit points, as shown in Fig. 6. There are two patterns in the figure. The prompt loss group and the group of numbers determined by the longer field lines. The prompt loss lines (those marked by 0) have a wider spread in the poloidal angle. Its extent is essentially determined by the radial extent of the starting locations. The spread in poloidal angle of the longer lines is intrinsic in nature and is proportional to the strength of the ergodic coils. It is interesting to note from more detailed examination reveals that there are no similarities between the hit point patterns left by the different length groups (6, 7, 8, or 9). The extent of their span in poloidal angle is nearly identical. As shown in the figure, this width is 4 deg poloidal angle or 8 cm in real space. This should be compared with 1 to 2 cm of the width of the heat load spread observed in axisymmetric H-mode plasma discharge in DIII-D. 8 cm is the additional width that the heat load from inside of the plasma can be expected to spread over. We note that the pattern in Fig. 6 has an  $n = 3$  toroidal sinusoidal variation. This sinusoidal pattern may be swept toroidally by a slow periodic time variation of a phased arrangement of the currents in a set of ergodic coils. In the inboard going direction, the pattern has a much narrower spread. It is approximately half of the outboard going spread. It is easy to deduce that the pattern on the floor is essentially determined by the magnetic field of the local X-point region. However, the entrance of a flux line into the loss region is random. This effect may be utilized to enhance the spread out of the heat flux on the divertor floor.



### 3. The “Window Pane” Coil

From the results of Section 2, we realized that the spread of the hit points on the divertor plate is mainly determined by the strength of the local perturbation magnetic field. We may enhance this effect by exciting currents in a set of “window pane” coils. The placement of the coil is only on the floor of the vessel. Their location being directly underneath the hit points and would then have a large effect on them. On the inscribed circle shown in Fig. 1, this set of coils give the harmonic content as shown in Fig. 7. The  $n = 3$  component is concentrated at  $m = 1$  with a narrow peak. The higher harmonic contents are small. With 27.5 kA in the coil, it has a 7.5 G,  $m = 1$  component on the inscribed circle. But since these mode numbers are not resonant with the  $q$  values near the separatrix, it has negligible effect in ergodizing the edge flux surfaces. It could, however, cause a large spread in the poloidal extent of the hit points on the divertor floor. Shown in Fig. 8 is the pattern of the length of the field lines as a function of the poloidal and toroidal angles of their hit points. Note that these are all prompt loss lines. The outer sinusoidal pattern is produced by trajectories with starting locations further from the separatrix. This sinusoidal spread increases as the starting locations move toward the separatrix from the outside. It is seen that this spread increases to 8 cm on the outboard side of the divertor floor for the field lines starting at the separatrix. This pattern is not random and it attests to the nearly non-ergodic nature of the plasma edge. The corresponding spread on the inboard side of the divertor floor is  $\sim 6$  cm, still substantial. Therefore, if we are interested mainly in moving the hit points on the floors alone, we could excite only these window pane coils.

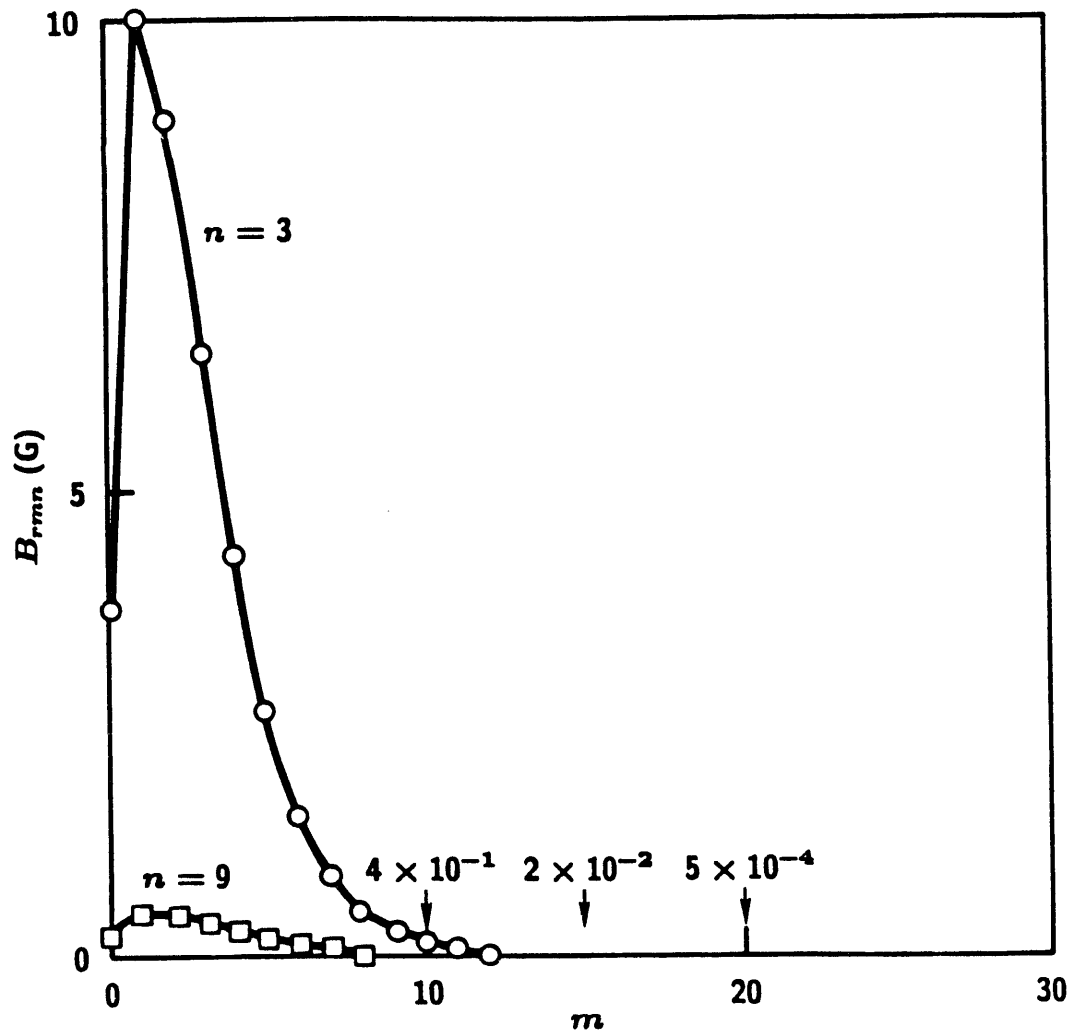


Fig. 7. Fourier amplitudes of the perturbation field produced by the window pane coil on the circle shown in Fig. 1 as a function of poloidal mode number for  $n = 3$  and  $n = 9$ .

### TOTAL-LEN-BOTH

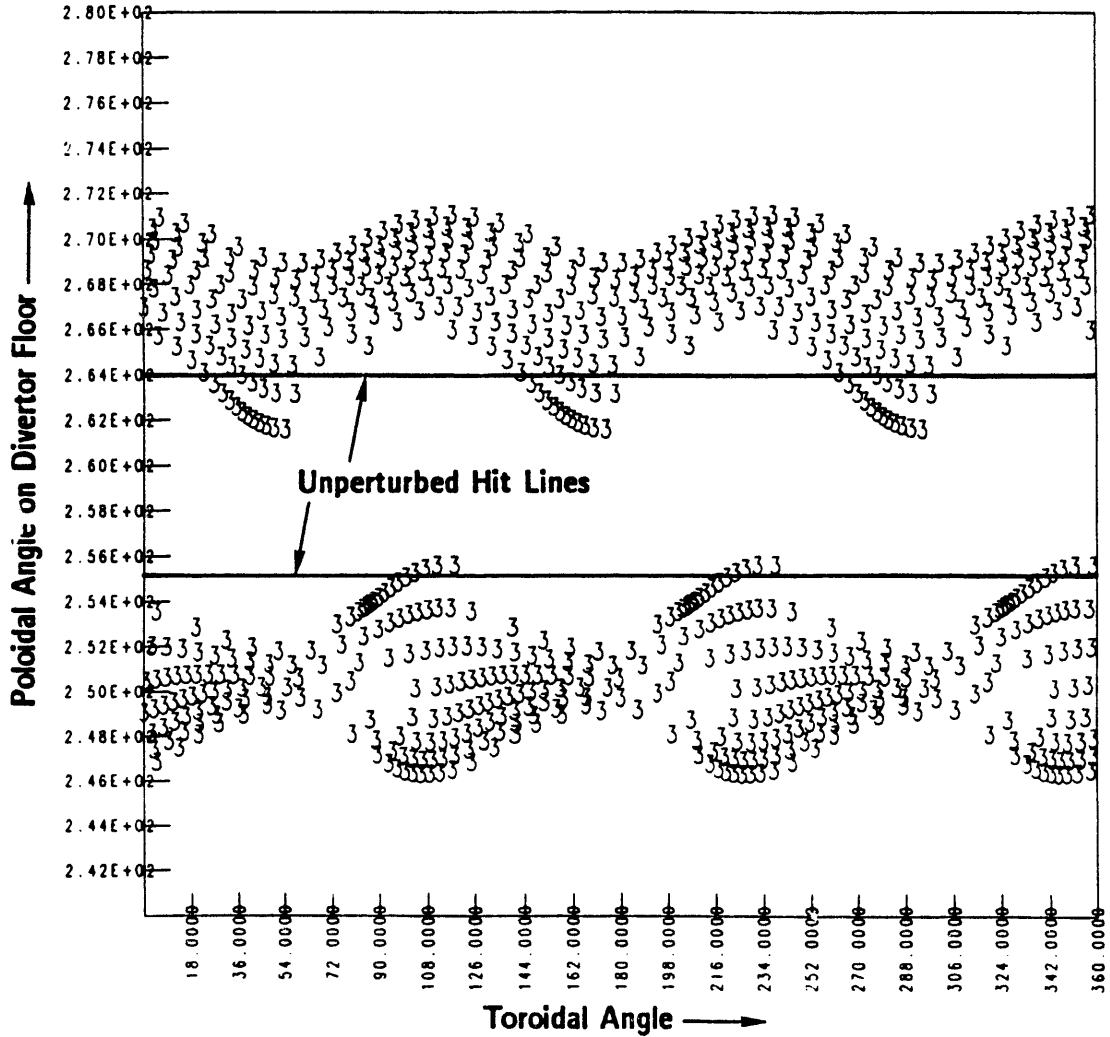


Fig. 8. The length of the lost field lines due to the effect of the window pane coils plotted as a function of the toroidal and poloidal angle of their hit points on the floor. Although the pattern is not stochastic, it has a large spread in the major radius direction.

## 4. A Combination of the Coils

From the above sections we recognized that we may perform two different kinds of perturbation to the plasma by placing coils around the X-point of a diverted plasma. We may ergodize the edge with very little effect on the inside by utilizing the helical coils and we may spread the heat out on the divertor plate by utilizing a large local field perturbation near the X-point. These two effects may be superimposed. Shown in Fig. 9 is the resultant midplane length plot of the field lines for 5 kA in the helical coils and 37.5 kA currents in the window pane coil. It is seen from this midplane pattern that the field lines are randomized. Examination of the hit point pattern on the floor reveals that it is made up of the composite effect from the two sets of coils. It has a large extent in its radial spread.

### OUTBOARD-GOING-LENGTH

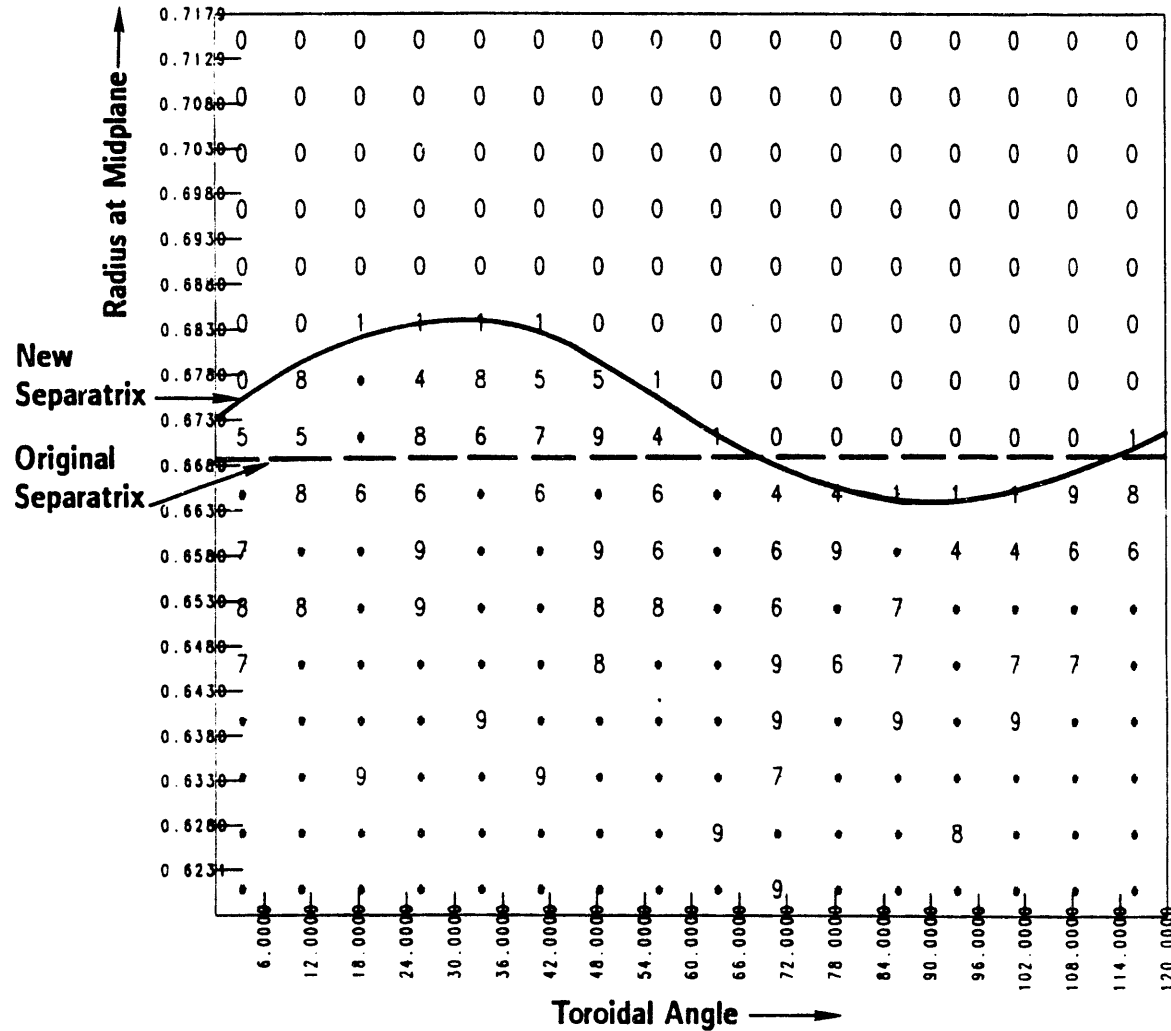


Fig. 9. Length of the field lines as a function of their starting position on the outboard midplane shown on a logarithmic scale. 5 kA of currents in the helical coil and 37.5 kA in the window pane coils are used. It is comparable to that shown in Fig. 5.

## 5. Conclusions

At the plasma edge, the plasma temperature is  $\sim 100$  eV. We have shown that relatively low current ergodic coils can be used to control the magnetic topology near the separatrix of DIII-D. This will provide a broadened scrape-off layer and reduce the peak heat deposition on the divertor targets by spreading out field line intersections with the target plates in DIII-D. In addition, it is known that relatively large toroidal and poloidal heat deposition asymmetries exist in tokamak because of small intrinsic magnetic perturbations [10]. Since toroidal asymmetries are particularly dangerous for divertor failures, it is reasonable to expect (as proposed in Ref. 10) that the ergodic layer can be used to reduce the effects of toroidal and poloidal asymmetries and to provide a greater degree of control and flexibility in the operation of the divertor. As an example, we calculate below the effect of the magnetic diffusion induced by our DIII-D coil design on the electron thermal diffusivity  $\chi_e$  and particle diffusion coefficient  $D_n$ . For a plasma temperature of 100 eV, the Bohm cross-field diffusion in a 30 kG toroidal magnetic field is  $2 \text{ m}^2/\text{sec}$ . In the example shown, the average migration of the field line after 1000 m in length is around 3 cm, which translates into a diffusivity of the magnetic field  $D_M$  as  $10^{-6} \text{ m}$ . At 100 eV, the electrons would have a thermal speed of  $4.3 \times 10^6 \text{ m/sec}$  and the hydrogen ion thermal speed is at  $10^5 \text{ m/sec}$  for  $T_e = T_i$ . By using the estimation of  $D = D_M v_{th}$ , we obtain  $\chi_e \simeq 4.3 \text{ m}^2/\text{sec}$  and  $D_n \simeq \chi_i \simeq 0.1 \text{ m}^2/\text{sec}$  by employing the test particle diffusion formula with the electron and ion thermal speeds at 100 eV, respectively. We would therefore expect the ergodic magnetic field to have an ability to cool the electron temperature at the edge and provide control to the edge plasma density for ELM control. Since the heat load on the divertor floor is expected to be spread out by the time-dependent modulation of the currents in the ergodic coils, the impurity production and backward migration problems into the main plasma will also be alleviated.

## 6. Acknowledgments

The authors would like to acknowledge useful discussion with Drs. J.M. Greene and D.N. Hill.

This is a report of work sponsored by the U.S. Department of Energy under Contract No. DE-AC03-89ER53277.

## 7. References

- [1] GOHIL, P., MAHDAVI, M.A., LAO, L., BURRELL, K.H., CHU, M.S., et al., *Phys. Rev. Lett.* **61** (1988) 1603.
- [2] POST, D.E., *Physics R and D Issues for CIT and ITER*, U.S. DOE, Germantown, Md. (1988).
- [3] ENGELHARDT, W., FENEBERG, W., *J. Nucl. Mater.* **76-77** (1978) 518.
- [4] PARKER, R., BATEMAN, G., COLESTOCK, P.L., FURTH, H.P., GOLDSTON, R.J., et al., in *Plasma Physics and Controlled Fusion Research* (Proc. 12th Int. Conf. Nice, 1988) IAEA, Vienna (1989) Vol. III, p. 341.
- [5] OHYABU, N., DEGRASSIE, J., *Nucl. Fusion* **27** (1987) 2171.
- [6] EVANS, T.E., GROSMAN, A., GUILHEM, D., HESS, W., LASALLE, J., et al., *Bull. Am. Phys. Soc.* **34** (1989) 2168, and TORE SUPRA DRFC/CAD Report No. EUR-CEA-FC 1394, July 1990.
- [7] SHOJI, T., FUJITA, T., MORI, M., HOWALD, A.M., LEONARD, A.W., et al., in *Controlled Fusion and Plasma Physics* (Proc. 17th Euro. Conf. Amsterdam, 1990), Part 3 (1990) 1452.
- [8] HILL, D.N., PETRIE, T.W., BROOKS, J.N., BUCHENAUER, D., FUTCH, A., et al., in *Plasma Physics and Controlled Fusion Research* (Proc. 13th Int. Conf. Washington, 1990) IAEA, Vienna (to be published) paper CN-53/G-1-3.
- [9] LA HAYE, R.J., *Nucl. Fusion* **31** (1991) 1550.
- [10] EVANS, T.E., NEUHAUSER, J., LEUTERER, F., MÜLLER, E.R., THE ASDEX TEAM, *J. Nucl. Mater.* **176 & 177** (1990) 202; EVANS, T.E., THE ASDEX TEAM, Max-Planck-Institut für Plasmaphysik Report No. IPP III/154, March 1991.

**END**

**DATE  
FILMED**

*12/05/91*